

Mathematics of pulsed vocalizations with application to killer whale biphonation

Judith C. Brown^{a)}

Physics Department, Wellesley College, Wellesley, Massachusetts 02481 and
Media Lab, Massachusetts Institute of Technology, Cambridge, Massachusetts 02139

(Received 19 August 2007; revised 18 January 2008; accepted 8 February 2008)

Formulas for the spectra of pulsed vocalizations for both the continuous and discrete cases are rigorously derived from basic formulas for Fourier analysis, a topic discussed qualitatively in Watkins' classic paper on "the harmonic interval" ["The harmonic interval: Fact or artifact in spectral analysis of pulse trains," in *Marine Bioacoustics 2*, edited by W. N. Tavogla (Pergamon, New York, 1967), pp. 15–43]. These formulas are summarized in a table for easy reference, along with most of the corresponding graphs. The case of a "pulse tone" is shown to involve multiplication of two temporal wave forms, corresponding to convolution in the frequency domain. This operation is discussed in detail and shown to be equivalent to a simpler approach using a trigonometric formula giving sum and difference frequencies. The presence of a dc component in the temporal wave form, which implies physically that there is a net positive pressure at the source, is discussed, and examples of the corresponding spectra are calculated and shown graphically. These have application to biphonation (two source signals) observed for some killer whale calls and implications for a source mechanism. A MATLAB program for synthesis of a similar signal is discussed and made available online. © 2008 Acoustical Society of America.
[DOI: 10.1121/1.2890745]

PACS number(s): 43.80.Ka [WWA]

Pages: 2875–2883

I. INTRODUCTION

Marine mammals, such as killer whales, produce a wide range of vocalizations, among which pulsed calls have the most interesting and complex spectra. In general the mathematical properties of these calls have been discussed qualitatively (Watkins, 1967), and the initial goal of this paper is to derive general formulas for the spectra of some common shapes of pulsed wave forms showing rigorously, for example, the reason for missing spectral lines.

The mathematics of pulsed calls can give important information on call production. An example is given for a killer whale sound with a treatment of biphonation or simultaneous sound production by two independent sources. For many of these calls the signal from one source is modulated by the signal from the other source in a nonlinear interaction (Tyson, 2006; Tyson *et al.*, 2007). In this case involving multiplication in the time domain, the spectrum is obtained from the convolution of the individual spectra in the frequency domain; it is shown that these results can also be understood with a simple trigonometric formula giving amplitude information as well as frequency shifts. It is interesting to compare to human speech production where the source is filtered by vocal cavities giving rise to convolution in the time domain and multiplication in the frequency domain.

Finally results are given from a MATLAB (made available on the internet) program which can simulate two independent sources with one signal modulating the other. The spectrum of the simulation is compared to that of a recorded

killer whale sound, and the implication of the dc components (net positive pressure) for a source mechanism is discussed.

II. BACKGROUND

A. Watkins

In 1967 Watkins published a seminal article on what he called the "harmonic interval." This included a treatment of the spectra of pulse trains with varying ratios R of period (of the pulse train) to width of the pulses comprising the pulse train. He called the fundamental frequency of the pulse train the pulse repetition rate. He then considered the case where this pulse train is multiplied by a sinusoid of higher frequency called the pulse tone (shifting the original spectrum up by this higher frequency) and discussed the spectra resulting from varying R and making the point that the repetition rate of the pulse train can be obtained from the spacing between spectral lines. He also discussed the symmetry of the temporal wave form and how this leads to missing lines (Fourier components) in the spectrum.

We will derive Watkins' results to give explicit formulas for Fourier analysis of continuous time wave forms and of the discrete Fourier transform for a digitized time wave form for cases of interest. As an aside we make a comparison to the identical problem in the spatial domain of diffraction by a variable number of slits. Our terminology will follow that of the more recent literature (Miller and Bain, 2000, and references therein) referring to Watkins' pulse train (or "burst pulse train") as the low frequency component (LFC) and to his pulse tone as the high frequency component (HFC). In the case of his pulse tone with sidebands, the spectrum is an example of convolution of the LFC and HFC spectra in the

^{a)}Electronic mail: brown@media.mit.edu

frequency domain and hence arises from the multiplication of the LFC and HFC in the time domain. Or equivalently, the LFC is amplitude modulating the HFC, which implies a non-linear interaction between the two sources.

B. Two-voiced and biphonic calls

In Watkins' work on marine mammals sounds he treats the simultaneous production of two signals. There are a number of examples of this phenomenon both in the animal world and in that of musical instruments. Bird calls (Suthers, 1990, 2006) with two signals are classified as two-voiced when there are two independent sources and biphonic when a single source emits two signals. Some musical instruments produce what are called multiphonics. For example, a brass player can play one note and sing another with the sum of these two producing a third frequency. With the flute and clarinet, the fingering can be changed to enhance a higher harmonic and make its amplitude comparable to that of the fundamental. Similarly with Tuvan throat singing, the shape of the vocal cavities are changed to selectively amplify a higher harmonic of the sound wave being produced and resulting in the perception of two voices.

Biphonation by a group of Northern resident killer whales has been included in a discussion of nonlinear sources (Tyson, 2006; Tyson *et al.*, 2007). Although it is probable that there are two sources for these sounds, no distinction in terminology has been made in the marine mammal literature between two voiced and biphonic sound production. Calculations on this same group of sounds are found in Brown and Miller (2006, Brown *et al.* (2006, 2007), Tyson (2006), Tyson *et al.* (2007), and Miller *et al.* (2007).

III. CALCULATIONS

Results of the following calculations are summarized in the upper section of Table I for the continuous time cases and in the lower section for the discrete calculations. Note the period P of the pulse train is the reciprocal of its frequency and is also referred to as the pulse separation in the case of a finite pulse train.

A. Continuous time

1. Fourier series: Pulse train of infinite length and finite width W

The case of a pulse train with period P and pulse width W is graphed in Fig. 1.

From Fourier series analysis for a periodic function of time $f(t)$ with period T , the k th Fourier coefficient a_k is

$$a_k = \frac{1}{T} \int_{-T/2}^{T/2} f(t) \exp(-jk2\pi t/T) dt. \quad (1)$$

With parameters W and P from Fig. 1 and using the fact that the function is zero outside the interval $(-W/2, W/2)$

$$a_k = \frac{1}{P} \int_{-W/2}^{W/2} f(t) \exp(-jk2\pi t/P) dt = \frac{1}{k\pi} \sin(k\pi W/P). \quad (2)$$

TABLE I. Summary of results. The upper part gives formulas for the spectra of continuous temporal wave forms with the lower part for the sampled wave forms. Note the symbol M for the number of pulses in the window is written as m_{\max} in the corresponding figures.

CONTINUOUS with PERIOD P (in seconds)				
Physical example	Length	Width of pulse	Magnitude formula in frequency domain	Figure
Diffraction grating	Infinite	W	$\frac{1}{k\pi} \sin(k\pi W/P)$	1 and 2
Diffraction grating	Infinite	δ	$\frac{1}{P} \sum_{k=-\infty}^{+\infty} \delta\left(\omega - k \frac{2\pi}{P}\right)$	
M slits	MP	δ	$\frac{\sin(\omega MP/2)}{\sin(\omega P/2)}$	3
M slits	MP	W	$\frac{\sin(\omega MP/2)}{\sin(\omega P/2)} \frac{\sin(\omega W/2)}{\omega/2}$	4
DISCRETE with PERIOD P (in samples)				
Length	Number of Pulse	Width of Pulse	Magnitude formula in Frequency domain	Figure
N	1	W	$\frac{\sin(\pi kW/N)}{\sin(\pi k/N)}$	
N	M	1	$\frac{\sin(\pi kMP/N)}{\sin(\pi kP/N)}$	5
N	M	W	$\frac{\sin(\pi kMP/N)}{\sin(\pi kP/N)} \frac{\sin(\pi kW/N)}{\sin(\pi k/N)}$	6 and 7

In the frequency domain this is the amplitude of the k th Fourier component and has radial frequency $k2\pi/P$, with frequency separation $2\pi/P$ (Watkins' "harmonic interval") of the components. The coefficients are plotted against k , the harmonic number, in the lower half of Fig. 1 for the case

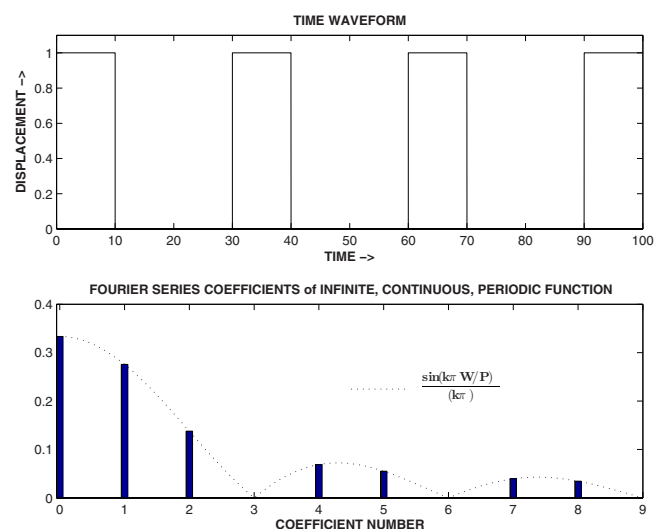


FIG. 1. (Color online) Temporal wave form (upper panel) and magnitude Fourier series coefficients (lower panel) of a pulse train with pulse width $W=10$ and pulse period $P=30$. Here $P/W=3$ and every third coefficient is missing. The dotted curve is the Fourier transform of a single pulse of width W and determines the amplitudes of the coefficients.

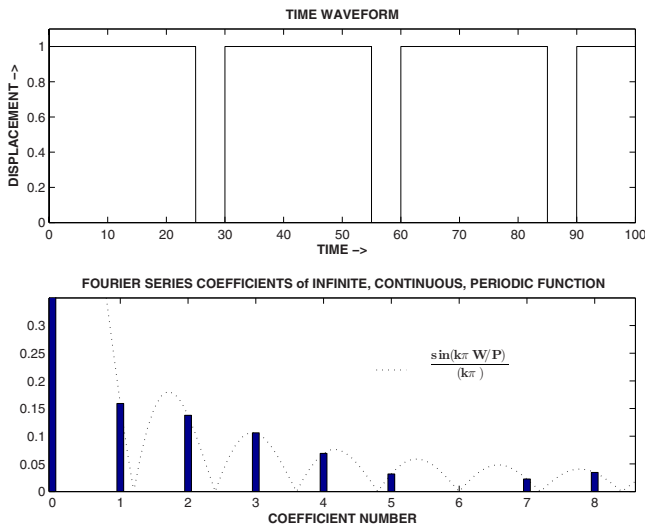


FIG. 2. (Color online) Temporal wave form (upper panel) and magnitude Fourier series coefficients (lower panel) of a pulse train with pulse width $W=25$ and pulse period $P=30$. Here $P/W=6$ to 5 and every sixth coefficient is missing. Note that the coefficients do not drop off as rapidly as in Fig. 1.

$P/W=3$, which shows clearly that every third Fourier coefficient is missing. Or in general for an arbitrary ratio P/W any coefficient which is a multiple of P/W will be missing. This is a simple, yet rigorous way to see Watkins' statements about missing spectral components. This case is equivalent in the spatial domain to a diffraction grating with slit width b and slit separation d (Brown, 1971).

Another case which has not been treated explicitly but is more widely applicable to pulsed animal vocalizations is that of the pulse width W greater than half the period P or P/W less than 2. The same formula applies for this case but the condition for missing Fourier components becomes

$$k\pi W/P = q\pi$$

with k and q integers or

$$kW/P = q.$$

This condition will be met for any k which is an integral multiple of P . The lowest value of k for which this can occur is $k=P$. This case is graphed in Fig. 2 for the case of $P=k=6$ and $W=5$. This can be interpreted (as seen in this graph) as the positions of integral k "beating" with the zeros of the amplitude function. The result is that there are fewer missing components and the radial frequency separation is $2\pi/P$ for most of the components. Physically, if the individual harmonics corresponding to each k value are graphed against time and compared to the time wave form, the missing components are those having maxima (or minima) at the beginning and end of the pulse, i.e., the transition from 0 to 1 or 1 to 0.

2. Fourier series: Pulse train of infinite length and negligible width

As the pulse width approaches zero, the ratio of P/W becomes very large with the central lobe (dotted curve in

Fig. 1 spreading to ∞ , and qualitatively one expects that the Fourier series coefficients will have equal amplitude with radial frequency separation $2\pi/P$.

More formally, the periodic function to be analyzed is an impulse train and can be written as a sum of delta functions,

$$f(t) = \sum_{m=-\infty}^{+\infty} \delta(t - mP)$$

giving

$$a_k = \frac{1}{P} \int_{-P/2}^{P/2} \delta(t) \exp(-jk2\pi t/P) dt = 1/P, \quad (3)$$

which is constant, independent of k as predicted, and has the same separation of components as in the previous case. Stated otherwise the transform of an impulse train of periodicity P in the time domain is an impulse train in the frequency domain with radial frequency separation $2\pi/P$, and equal to $1/P \sum_{k=-\infty}^{+\infty} \delta(\omega - k2\pi/P)$.

3. Fourier transform: Impulse train of finite length

Changing from an infinite impulse train to a finite one, the Fourier series gives rise to the Fourier transform given by

$$g(\omega) = \int_{-\infty}^{\infty} f(t) \exp(-j\omega t) dt. \quad (4)$$

Considering a finite impulse train with period P and M pulses

$$f(t) = \sum_{m=0}^{M-1} \delta(t - mP).$$

Substituting in Eq. (4),

$$g(\omega) = \int_{-\infty}^{\infty} \sum_{m=0}^{M-1} \delta(t - mP) \exp(-j\omega t) dt = 1 + \exp(-j\omega P) + \cdots + \exp(-j(M-1)\omega P) = \sum_{m=0}^{M-1} \exp(-jm\omega P). \quad (5)$$

This is a geometric series with sum:

$$g(\omega) = \frac{1 - \exp(-j\omega MP)}{1 - \exp(-j\omega P)} = \frac{\sin(\omega MP/2)}{\sin(\omega P/2)} \exp(j\omega P/2 - j\omega MP/2), \quad (6)$$

where the phase factor can be dropped in a consideration of spectral magnitudes. An example for the case of $M=5$ is found in Fig. 3.

4. Fourier transform: Pulse train of finite length and pulse width W

The Fourier transform can be obtained by considering a time wave with M pulses of width W and integrating in Eq. (4) directly. This case is treated in texts on physical optics for M slits with finite width b in the spatial domain. See, for

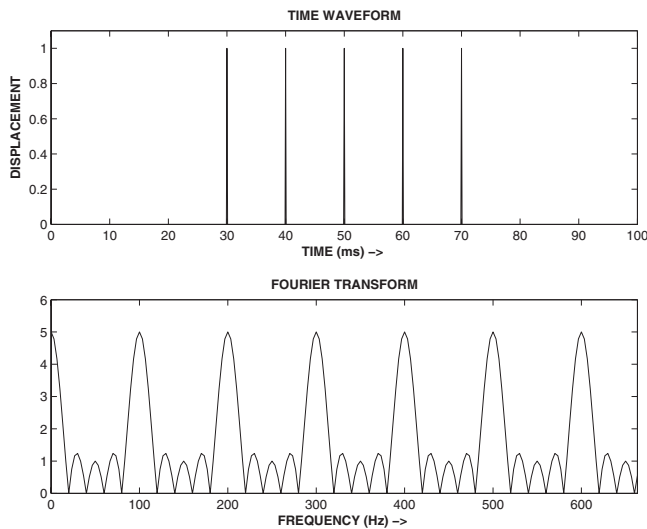


FIG. 3. Temporal wave form (upper panel) and magnitude Fourier transform (lower panel) of a finite impulse train. Here there are five impulse functions with separation $P=10$.

example, [Jenkins and White \(1976\)](#). It is simpler and will provide a useful tool for later sections to use the convolution theorem ([Oppenheim et al., 1983](#)) which states that, if two functions are convolved in the time domain, their Fourier transform is the product of their individual transforms (and conversely from frequency domain to time domain).

The time wave form describing the pulse train is the convolution of the finite impulse train from the previous section and a single pulse of width W . The convolution is identical to a cross correlation except that one function is time reversed. The result is the temporal wave form for the example of five pulses of width W equal to 3.33 ms shown in Fig. 4.

To obtain the Fourier transform, we need the transforms from Eq. (6) and the transform of a single pulse of width W .

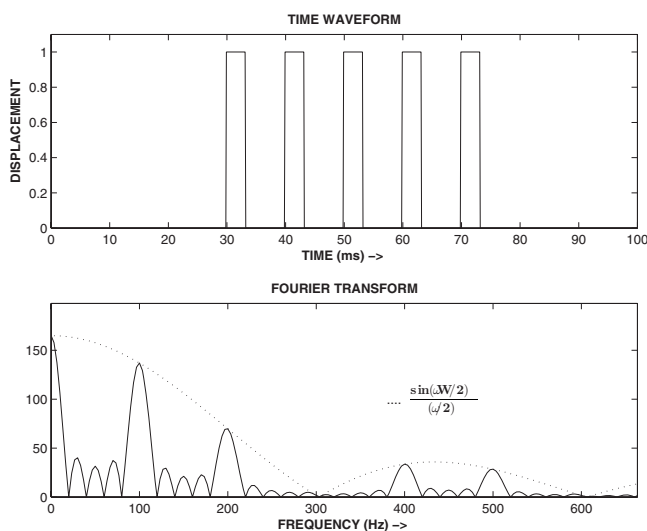


FIG. 4. Temporal wave form (upper panel) and magnitude Fourier transform (lower panel) of a finite pulse train with five pulses having pulse separation 10 and pulse width 3.33 such that $P/W=3$ as in Fig. 1. Here there are secondary maxima between the principal maxima, but as in Fig. 1 every third principal maximum is missing.

The latter can be obtained using Eq. (4) to evaluate an integral identical to that of Eq. (2) with the result:

$$g(\omega)_{\text{pulse}} = \frac{\sin(\omega W/2)}{\omega/2}. \quad (7)$$

This is the dotted function plotted in the lower half of Fig. 4 (scaled to match the maximum of the solid curve).

Using the convolution theorem to obtain the transform we multiply the transforms from Eqs. (6) and (7) to obtain

$$|g(\omega)| = \frac{\sin(\omega MP/2)}{\sin(\omega P/2)} \frac{\sin(\omega W/2)}{\omega/2}. \quad (8)$$

This is the function plotted with a solid line in the lower half of Fig. 4. Clearly it is the product of the transform of a single pulse of width W with that of the five impulses plotted in Fig. 3. In the spatial domain this formula describes diffraction by M slits with width b corresponding to W .

B. Discrete time: Discrete Fourier transform implemented with fast Fourier transform

The previous calculations for the continuous time cases are interesting and instructive; and they form a basis for the derivation and understanding of the formulas describing implementation of the discrete Fourier transform (DFT) as a fast Fourier transform (FFT) on a sampled wave form.

Traditional notation is followed in considering a window of N samples of a function $x[n]$. For comparison with Section A above, the pulse trains will have period P and width W , but now in units of samples. If desired these quantities can be converted to seconds by dividing by the sample rate, which is 100 in the examples.

For any window of N samples of the function $x[n]$, the inverse of its DFT will be replicated with periodicity N (whatever the shape or periodicity of $x[n]$), and the DFT, $X[k]$, has periodicity in the frequency domain equal to the sample rate. Since the magnitudes of $X[k]$ and $X[-k]$ are equal, there are $N/2$ unique magnitudes of the Fourier components. Note that a rectangular window is assumed in the following examples to make them tractable algebraically. Most software packages include the option of multiplying by a windowing function; this effect can be obtained by a convolution in the frequency domain of the Fourier transform of the window function with the formulas which are derived in the following ([Harris, 1978](#)).

1. Discrete Fourier transform: Single pulse of width W

Consider first a single pulse of width W samples. The general expression for the discrete Fourier transform is ([Oppenheim and Schaffer, 1975](#))

$$X[k] = \sum_{n=0}^{N-1} x[n] \exp(-j2\pi kn/N). \quad (9)$$

Here $x[n]=1$ for $0 \leq n \leq W-1$ and 0 over the remaining interval, and $X[k]$ is the k th Fourier component with angular frequency $2\pi k/N$ in units of radians/sample. Substituting for $x[n]$,

$$X[k] = \sum_{n=0}^{W-1} \exp(-j2\pi kn/N).$$

This is a geometric series identical to that evaluated following Eq. (5) and gives

$$|X[k]| = \frac{\sin(\pi kW/N)}{\sin(\pi k/N)} \quad (10)$$

for $k=0$ to $N/2-1$ magnitudes. Its shape can be seen as the dotted curve at the top of Fig. 6. It is interesting to compare this formula to Eq. (2). Here the window length N appears instead of P the period of the pulse train; and in the denominator a sin function appears replacing the argument alone. Both functions in Eq. (10) show that there is an overall periodicity in N due to sampling.

2. Discrete Fourier transform: Impulse train

Consider a windowed region $x_N[n]$ of the function $x[n]$ containing M impulses with spacing P . With the restriction that the first impulse occurs at the origin, M is the quotient of N/P rounded down to an integer, i.e., the number of complete periods in the window. Then

$$x_N[n] = \sum_{m=0}^{M-1} \delta(n - mP).$$

Substituting in Eq. (9)

$$X[k] = \sum_{n=0}^{N-1} \sum_{m=0}^{M-1} \delta(n - mP) \exp(-j2\pi kn/N). \quad (11)$$

This double sum can be evaluated as described leading to Eq. (6) with $2\pi k/N$ replacing ω . The result is

$$|X[k]| = \frac{\sin(\pi kMP/N)}{\sin(\pi kP/N)}. \quad (12)$$

Equation (12) is plotted at the top of Fig. 5 with points corresponding to integral k indicated. The middle graph is the sampled impulse train (chosen so that the impulse falls on a sampled point), and the bottom graph is the FFT of this impulse train with integral k points taken from the formula to demonstrate its accuracy as well as showing exactly how the calculated DFT samples compare to the function. Note that M in Eq. (12) corresponds to m_{\max} in the formula in the figure.

3. Discrete Fourier transform: General case—pulse train with M pulses of width W and period P

This is the sampled analog of M pulses of width W treated previously. As discussed the input pulse train is the convolution of the function representing M impulses and that for a single pulse of width W . As before, the transform is the product of their transforms, and the results from sub sections 1 and 2 above give

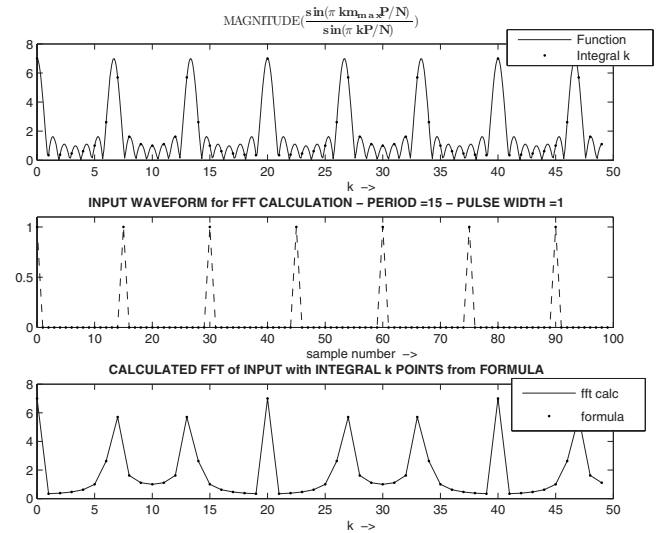


FIG. 5. Upper panel: Calculated magnitude function for the DFT of a sampled impulse train with period 15 samples. The points corresponding to integral k are indicated with a dot. Middle panel: Input wave form for the calculation, chosen so that samples occur at the maxima. Samples are indicated with a dot and connected with dashes. Lower panel: Actual calculation of FFT on samples in the middle panel. The points correspond to the samples for integral k indicated for the function in the top panel.

$$|X[k]| = \frac{\sin(\pi kMP/N)}{\sin(\pi kP/N)} \frac{\sin(\pi kW/N)}{\sin(\pi k/N)}. \quad (13)$$

Examples for ratios of pulse period to pulse width of 3 to 1 and 5 to 4 are plotted in Figs. 6 and 7. These can be compared to the continuous cases of Figs. 1 and 2.

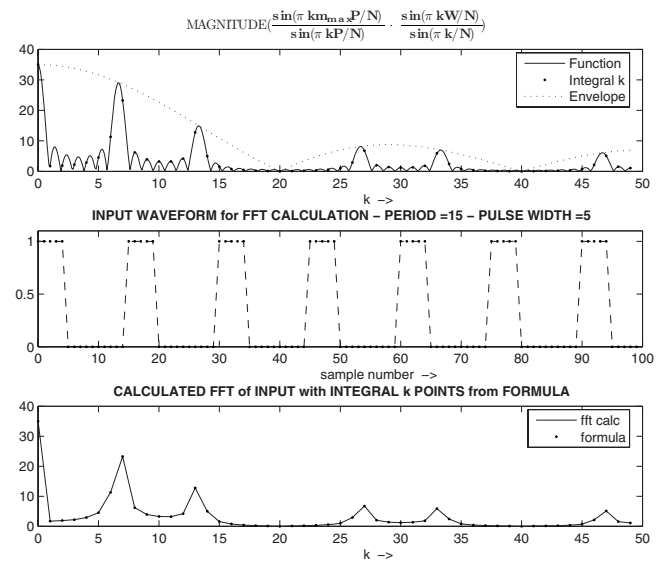


FIG. 6. Upper panel: Magnitude function for the DFT of a sampled pulse train with period 15 samples and pulse width 5 samples. The points corresponding to integral k are indicated with a dot. Middle panel: Input wave form for the calculation. Samples are indicated with a dot and connected with dashes. Lower panel: Actual calculation of FFT on samples from the input wave form. The points correspond to the samples for integral k indicated for the function in the top figure.

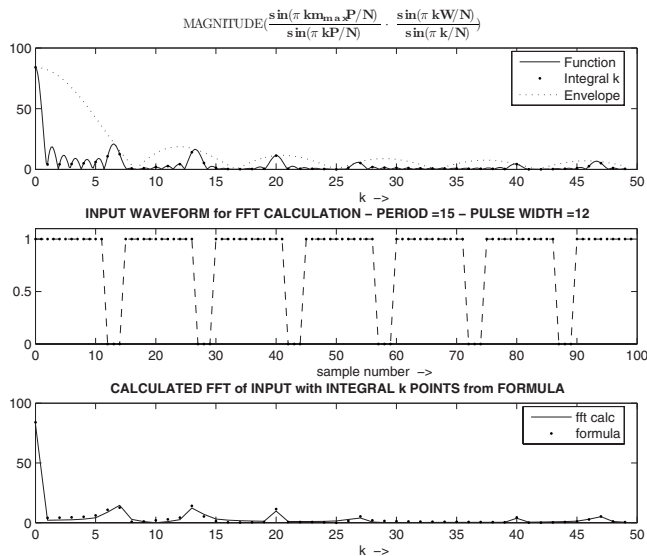


FIG. 7. Upper panel: Magnitude function for the DFT of a sampled pulse train with period 15 samples and pulse width 12 samples. The points corresponding to integral k are indicated with a dot. Middle panel: Input wave form for the calculation. Samples are indicated with a dot and connected with dashes. Lower panel: Actual calculation of FFT on the samples from the input wave form. The points correspond to the samples for integral k indicated for the function in the top figure.

C. Product of two signals

It is of interest to compare to the case of the sum of two signals having, for example, frequencies of ω_L and ω_H . Taking the transform is a linear operation, and the spectrum consists of two lines at these frequencies, i.e., the superposition of their individual transforms. Far more interesting effects occur for the nonlinear case of a product.

1. Convolution in the frequency domain

We can now consider Watkins' case of a pulse train spectrum shifted by the presence of a pulse tone, which corresponds to the multiplication of two signals. As pulse train we take the example from Fig. 2 with ratio of pulse period to pulse width of 6 to 5, and for clarity multiply it by a single sinusoid of higher frequency. The result is found in Fig. 8 where the sinusoid has frequency 1000 Hz and the pulse train has frequency 100 Hz. The effect in the frequency domain of this multiplication in the time domain is to shift the center of the spectrum of the pulse train from dc to 1000 Hz.

This is an example of multiplication in the time domain giving rise to convolution in the frequency domain. When we convolve the spectrum of the pulse train with the spectrum of the sinusoid (a single peak at 1000 Hz), each of the peaks of the original spectrum is shifted up in frequency by 1000 Hz. This can also be "derived" from the trigonometric identity:

$$\begin{aligned} \cos(\omega_L t)\cos(\omega_H t) &= 1/2[\sin((\omega_L + \omega_H)t) \\ &\quad + \sin((\omega_H - \omega_L)t)]. \end{aligned} \quad (14)$$

Each component ω_L of the pulse train will appear as its sum and difference with ω_H , the higher frequency. Or in other words ω_H acts as the new baseline, and since ω_L rep-

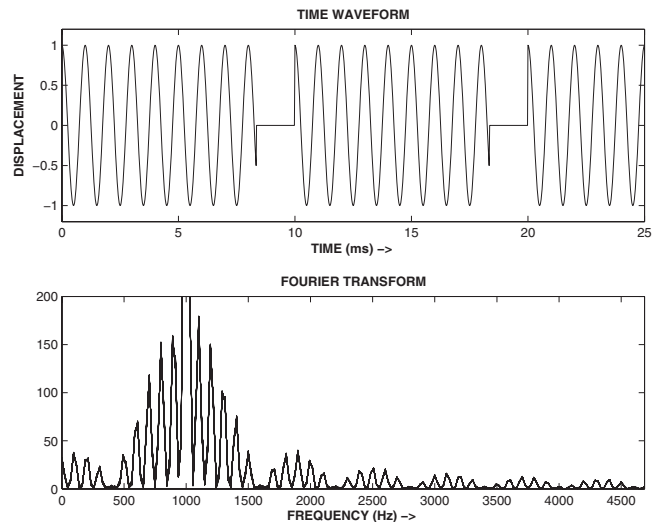


FIG. 8. Upper panel: Wave form of a sinusoid of frequency 1000 Hz multiplied by a pulse train of frequency 100 Hz having a ratio of pulse period to pulse width of 6 to 5. Lower panel: Fourier transform of the above wave form showing that the spectrum of the pulse train is shifted up in frequency by 1000 Hz.

resents any of the components of the pulse train, the entire spectrum with positive and negative frequency components is shifted upwards by ω_H .

Since the spacing of the components relative to each other is preserved, this gives rise to Watkins' statement that the pulse repetition rate can be obtained from the separation between harmonic bands.

2. Importance of the dc component

The displacement in Fig. 2 is positive with respect to a zero baseline and thus has a positive average. With this duty cycle it is a fairly high number. This is reflected in the frequency domain by the center component at 1000 Hz in Fig. 8 which goes off scale. Note that the unshifted spectrum of this pulse train would look like that of Fig. 2 (also having an offscale dc component).

Figure 9 shows the effect of a dc component on the spectrum of two sinusoids (chosen for simplicity), which are multiplied. The upper and middle parts of Fig. 9 show the LFC and HFC with a dc component turned on and off and its appearance and disappearance in the spectrum. The spectrum is plotted against time to show this more clearly. At the bottom of Fig. 9 is found the product of these two functions with and without a dc component.

To examine the lower part of Fig. 9 quantitatively, Eq. (14) can be modified to include a dc component A_{oL} and A_{oH} for each of the individual components (now with amplitudes A_{ω_L} and A_{ω_H}) to give

$$\begin{aligned} (A_{oL} + A_{\omega_L} \cos(\omega_L t))(A_{oH} + A_{\omega_H} \cos(\omega_H t)) &= A_{oL}A_{oH} \\ &\quad + A_{oH}A_{\omega_L} \cos(\omega_L t) + A_{oL}A_{\omega_H} \cos(\omega_H t) \\ &\quad + (1/2)A_{\omega_L}A_{\omega_H}[\sin((\omega_L + \omega_H)t) + \sin((\omega_H - \omega_L)t)]. \end{aligned} \quad (15)$$

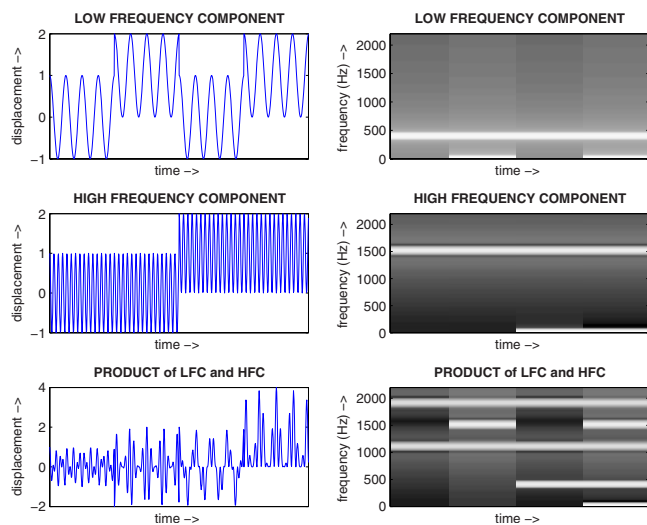


FIG. 9. (Color online) Upper panel: Wave form (left) and spectrum (right) of a low frequency sinusoid with and without a dc component. Middle panel: Wave form and spectrum of a higher frequency sinusoid with and without a dc component. Lower panel: Wave form and spectrum of the product of the wave forms in the upper and middle panels.

From Fig. 9, it is clear that to have a component at the center frequency ω_H of the shifted spectrum, there must be a dc component present for the LFC. This corresponds to the third term on the right in Eq. (15). And to see the unshifted spectrum of the LFC in Fig. 9, there must be a dc component for the HFC; this corresponds to the second term on the right. The strength of the sum and difference terms is independent of the presence of dc terms and is equal to the product of their individual amplitudes, shown in the last two terms. They should appear symmetrically around the center frequency (i.e., the frequency of the HFC).

The presence of a dc component is physically meaningful as it implies a net positive pressure at the source. A biological example of this effect in sound production for an anuran (frogs and toads) is discussed in Bradbury and Vehrencamp (1998). An example for a killer whale having a dc component for both the LFC and the HFC follows in Sec. IV. The discussion presented above can then apply, by extension, to any two spectral lines from the more complex sounds originating from two real sources.

IV. BIPHONATION EXAMPLES

A. Killer whale

An example of a Northern resident killer whale called type n32 (cataloged by Ford, 1987) is found in Fig. 10. This is one of a set of calls recorded off Vancouver Island, Canada in 1998 and 1999 using a beamforming array (Miller and Tyack, 1998; Miller *et al.*, 2007). Digital recordings were made with Tascom recorder with a 48 kHz sampling rate and 16 bit samples.

This is an excellent example of a call where the HFC has a fundamental and two upper harmonics (and probably more that go off scale). Here the spectrum of the LFC can be seen with respect to dc and then shifted up by the frequency of each line in the spectrum of the HFC. Note the negative

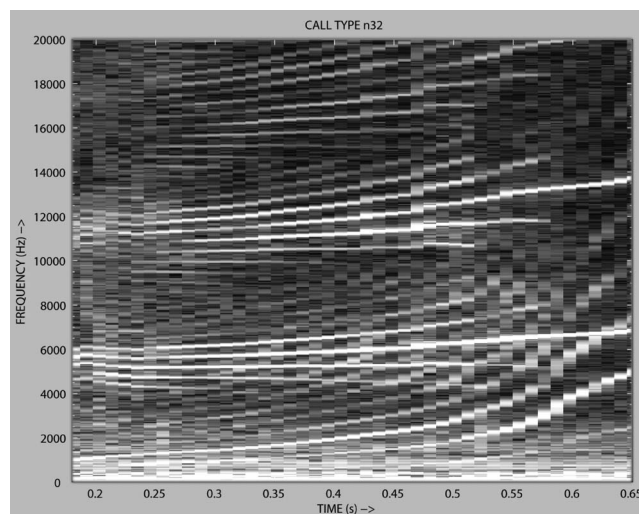


FIG. 10. Example of a Northern resident killer whale call of type n32 with a rising low frequency component having a number of harmonics and a high frequency component (HFC) with fundamental starting around 5800 Hz and rising slowly. The HFC also has a second and third harmonic visible.

frequency components of the LFC appear as mirrored by each HFC harmonic. The LFC has a number of harmonics, which can be seen most clearly after 0.5 s where the fundamental frequency is rising and its harmonics 3, 4, and 5 intersect the fundamental of the HFC.

This is an excellent example of the relevance of the previous discussion of the dc components since the unshifted spectrum of the LFC is present and indicates a dc component for the HFC. Also the center line of the LFC is seen at the frequency of each of the harmonics of the HFC, indicating a dc component for the LFC. This is somewhat counterintuitive but follows from Eq. (15). If the unshifted LFC spectrum is present, it means there is a dc component for the HFC; and if the spectral lines of the HFC are present (rather than just seeing the LFC mirrored about a central position), it means that there is a dc component of the LFC.

B. Synthetic signal

As a test of the analysis of the call of Fig. 10, a MATLAB program¹ was written to synthesize a similar sound. A model of the low frequency call consists of a pulse train similar to that of Fig. 2 with fundamental frequency varying from 450 to 900 Hz. This was filtered to drop off at around 3000 Hz for less overlap with components due to the HFC. The shape of this LFC is shown with the dotted line of Fig. 11 on the left.

The HFC consists of a fundamental varying from 5800 to 6500 Hz with second and third harmonics each having amplitudes reduced by a factor of 10. Two periods of the product of the LFC and HFC are shown in the time wave at the left of Fig. 11. The spectrum is given on the right side of Fig. 11 and is the convolution of the individual (not shown but easily inferred) LFC and HFC spectra as predicted.

The Fourier transform as a function of frequency is shown in Fig. 12 and shows amplitudes which can be inferred from Eq. (15). For example, each of the sum and difference lines has the same amplitude. This is not rigor-

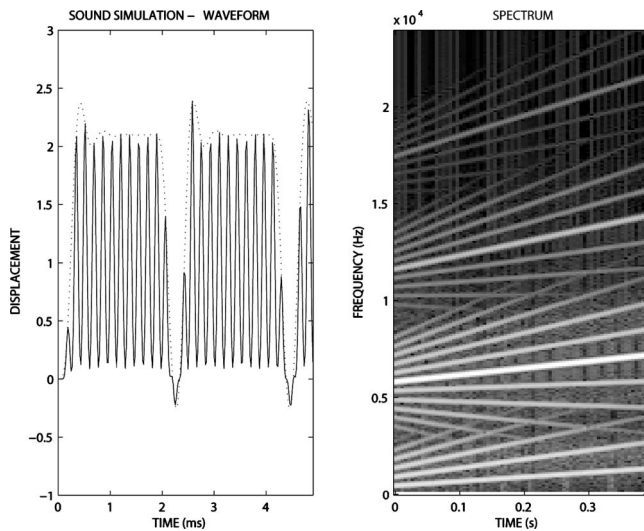


FIG. 11. Simulation of the wave form (left) and spectrum (right) of the killer whale call of Fig. 10. The wave form is the product of an HFC with fundamental varying from 5800 to 6500 Hz and a LFC (dotted) with ratio of period to pulse width of 6 to 5. The LFC is filtered to drop off at around 3000 Hz for less overlap, and this gives rise to the distortion of the square pulse.

ously true for the killer whale sound of Fig. 10 and thus implies some formant structure in the killer whale production anatomy amplifying spectral regions selectively.

V. DISCUSSION

The mathematics of pulsed calls can give important information on call production. For calls such as the example given for the killer whale, the fact that there is a convolution in the frequency domain implies that there are two sources and that they are interacting nonlinearly. This means that they are multiplied, and the LFC is amplitude modulating the HFC. The presence of dc components for each source implies a net positive pressure for each source.

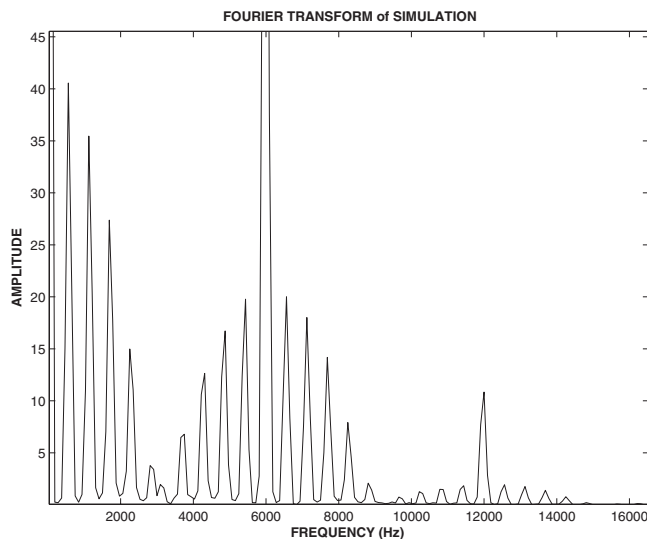


FIG. 12. Magnitude of the Fourier transform for the simulation in Fig. 11 at time 0.05 s plotted against frequency.

These observations support a source mechanism for odontocetes proposed by Cranford and others (Cranford *et al.*, 1996; Cranford, 2000; 2006) in a series of papers over the past decades. Two sets of phonic lips (also called monkey lips dorsal bursae complexes or MLDB) are set in vibration by two independent sources of air under pressure in the nasal passages implying a net positive pressure as discussed earlier. The vibrations are independent despite the experimental observation that the pressure in the two nasal passages does not differ (Cranford, 2006) for the case of the bottlenose dolphin. These vibrations may be coupled through the dorsal bursae to the melon which acts as an acoustic lens and impedance match to the ocean water.

As postulated the two sources would produce independent vibrations, and the spectrum would be that of the sum of those due to the individual vibrations. This is in fact observed for many killer whale calls (Hodgins-Davis, 2004). Others (see Fig. 1 in Miller *et al.*, 2007) show a nonlinear coupling, though in general it is less strong than that of Fig. 10. Qualitatively the MLDB complexes are located near each other and the motion of one could easily affect the vibration of the other leading to the observed nonlinearity (Fletcher, private communication, 2007). It would be very interesting to see a theoretical treatment of this effect.

ACKNOWLEDGMENTS

I would like to thank Patrick Miller for the killer whale sound in Fig. 10 as well as Neville Fletcher and Ted Cranford for some interesting “electronic” discussions on a source mechanism.

¹MATLAB code can be obtained from <http://www.media.mit.edu/~brown>

- Bradbury, J. W., and Vehrencamp, S. L. (1998). *Principles of Animal Communication* (Sinauer Associates, Sunderland, MA).
- Brown, J. C. (1971). “Spatial filtering and fourier analysis,” *Am. J. Phys.* **39**, 797–801.
- Brown, J. C., Hodgins-Davis, A., and Miller, P. J. O. (2006). “Classification of vocalizations of killer whales using dynamic time warping,” *J. Acoust. Soc. Am.* **119**, EL34–EL40.
- Brown, J. C., and Miller, P. J. O. (2006). “Classifying killer whale vocalization using time warping,” *Acoustics Today* **16**, 45–47.
- Brown, J. C., and Miller, P. J. O. (2007). “Automatic classification of killer whale vocalizations using dynamic time warping,” *J. Acoust. Soc. Am.* **122**, 1201–1207.
- Cranford, T. (2006). “Odontocete nasalizations: Morphology, physiology, and evolution of sonar signal generation in toothed whales,” *J. Acoust. Soc. Am.* **120**, 3189–3190.
- Cranford, T. W. (2000). “In search of impulse sound sources in Odontocetes,” in *Hearing by Whales and Dolphins*, edited by W. W. L. Au, A. N. Popper, and R. R. Fay (Springer, New York), pp. 109–155.
- Cranford, T. W., Amundin, M. E., and Norris, K. S. (1996). “Functional morphology and homology in the odontocete nasal complex: Implications for sound generation,” *J. Morphol.* **228**, 223–285.
- Ford, J. K. B. (1987). “A catalogue of underwater calls produced by killer whales (*Orcinus orca*) in British Columbia,” *Can. Data Rep. Fish. Aq. Sci.* No. 633.
- Harris, F. J. (1978). “On the use of windows for harmonic analysis with the discrete Fourier transform,” *Proc. IEEE* **66**, 51–83.
- Hodgins-Davis, A. (2004). “An analysis of the vocal repertoire of the captive killer whale population at marineland of Antibes, France,” thesis, Wellesley College, Wellesley, MA.
- Jenkins, F. A., and White, H. E. (1976). *Fundamentals of Optics*, 4th ed. (McGraw-Hill, New York).
- Miller, P. J. O., and Bain, D. E. (2000). “Within-pod variation in the sound

- production of a pod of killer whales, *Orcinus orca*,” *Anim. Behav.* **60**, 617–628.
- Miller, P. J. O., Samarra, F. I. P., and Perthuison, A. (2007). “Caller sex and orientation influence spectra of ‘two-voice’ stereotyped calls produced by free-ranging killer whales,” *J. Acoust. Soc. Am.* **121**, 3932–3937.
- Miller, P. J. O., and Tyack, P. L. (1998). “A small towed beamforming array to identify vocalizing resident killer whales (*Orcinus orca*) concurrent with focal behavioral observations,” *Deep-Sea Res., Part II* **45**, 1389–1405.
- Oppenheim, A. V., and Schaffer, R. W. (1975). *Digital Signal Processing* (Prentice-Hall, Englewood Cliffs, NJ).
- Oppenheim, A. V., Wilsky, A. S., and Young, I. T. (1983). *Signals and Systems* (Prentice-Hall, Englewood Cliffs, NJ).
- Suthers, R. A. (1990). “Contributions to birdsong from the left and right sides of the intact syrinx,” *Nature (London)* **347**, 473–477.
- Suthers, R. A., Beckers, J. G. L., and Nelson, B. S. (2006). “Vocal mechanisms for avian communication,” in *Behavior and Neurodynamics for Auditory Communication*, edited by J. Kanwal and G. Ehret (Cambridge University Press, Cambridge), pp. 3–35.
- Tyson, R. B. (2006). “The presence and potential functions of nonlinear phenomena in cetacean vocalizations,” thesis, Florida State University, Tallahassee, FL.
- Tyson, R. B., Nowacek, D. P., and Miller, P. J. O. (2007). “Nonlinear phenomena in the vocalizations of North Atlantic right whales (*Eubalaena glacialis*) and killer whales (*Orcinus orca*),” *J. Acoust. Soc. Am.* **122**, 1365–1373.
- Watkins, W. A. (1967). “The harmonic interval: Fact or artifact in spectral analysis of pulse trains,” in *Marine Bioacoustics 2*, edited by W. N. Tavogla (Pergamon, New York), pp. 15–43.